Article

JOURNAL OF THE CHINESE CHEMICAL SOCIETY

A New, Highly Potent 1,8-Naphthalimide-based Fluorescence "Turn off" Chemosensor Capable of Cu^{2+} Detection in China's Yellow River Water Samples

Stephen Opeyemi Aderinto *

School of Chemical and Biological Engineering, Lanzhou Jiaotong University, Lanzhou, Gansu 730070, China

(Received: September 5, 2017; Accepted: October 25, 2017; DOI: 10.1002/jccs.201700308)

A new 1,8-naphthalimide-based fluorescence "turn off" chemosensor, *N*-phenyl-4-(3,3′-((2-aminoethyl)azanediyl)dipropanoic acid)-1,8-naphthalimide (**MAST**), for the detection of Cu^{2+} was synthesized. Upon treatment with Cu^{2+}, in coexistence with various competitive metal ions in HEPES-buffered dimethylsulfoxide (DMSO) solution (v/v, 1:1; pH 7.4), **MAST** displayed a high selectivity toward Cu^{2+} with a fluorescence quenching of 83.67%. Additionally, a good linear response of **MAST** for the detection of Cu^{2+} was obtained in the concentration range of 10×10^{-6} to 50×10^{-6} M. A 1:1 stoichiometric interaction of **MAST** with Cu^{2+} was observed, and the association constant and detection limit were calculated to be 1.37×10^{6} and 0.69×10^{-8} M, respectively. The sensing mechanism of the chemosensor toward Cu^{2+} was proposed due to the effect of the paramagnetic nature of Cu^{2+} and reverse-photo-induced electron transfer (PET) process. Ultimately, the proposed chemosensor was applied to quantify Cu^{2+} in real-world water samples, with excellent recovery rates of 98.00–109.80% observed.

Keywords: 1,8-Naphthalimide; Fluorescence "turn off" chemosensor; Cu^{2+}; Paramagnetic; Reverse-photo-induced electron transfer process.

INTRODUCTION

Over the past few decades, massive efforts have been taken toward the constructions of chemosensors for the monitoring of metal ions of biological and environmental importance.[1–10] In spite of the crucial roles metal ions play in environmental and biological systems, their ecotoxicological impingements have constituted great challenges for a long time.[11,12] More and more attention is being focused on the construction of chemosensors for Cu^{2+} due to the critical roles it plays by acting as a catalyst cofactor for some biologically important proteins involved in growth and development in the human body.[13–15] Abnormal thresholds of Cu^{2+} homoeostasis in human bodies are usually linked with some neurodegenerative diseases, including Wilson's disease, dyslexia, hypoglycemia, Alzheimer's disease, Menkes disease, Parkinson's disease, amyotrophic lateral sclerosis, infant liver damage, and gastrointestinal disease.[16–22] The toxicity data and scientific studies conducted by the World Health Organization (WHO) and US Environmental Protection Agency (US EPA) provided acceptable bearable limits of Cu^{2+} in drinking water at concentration levels of 31.5 and 20 μM, respectively.[14,23] Therefore, the selective monitoring of Cu^{2+} in both biological and environmental systems has become a subject of much relevance in the field of sensing science.

The early available methods of metal ion detection include atomic absorption spectrometry, inductively coupled plasma-atomic emission spectrometry, and inductively coupled plasma-mass spectrometry. Despite their merits, the constraints of difficulty, high cost of equipment, and time-consuming and demanding procedures still place some barriers on their applications.[24,25] Compared to these methods, the fluorescence technique has the superior features of high selectivity and sensitivity, simplicity of operation, low instrumentation cost, and rapid analytical detection, thereby making it a much better sensing technique.[26,27] The 1,8-naphthalimide and its derivatives have been widely exploited as exquisite, sought-after fluorophore moieties for chemosensors' construction due to their desirable qualities of excellent photophysical fluorescent properties of high photostability and quantum yield, strong

*Corresponding author. Email: 2014bsz528@stu.lzjtu.edu.cn

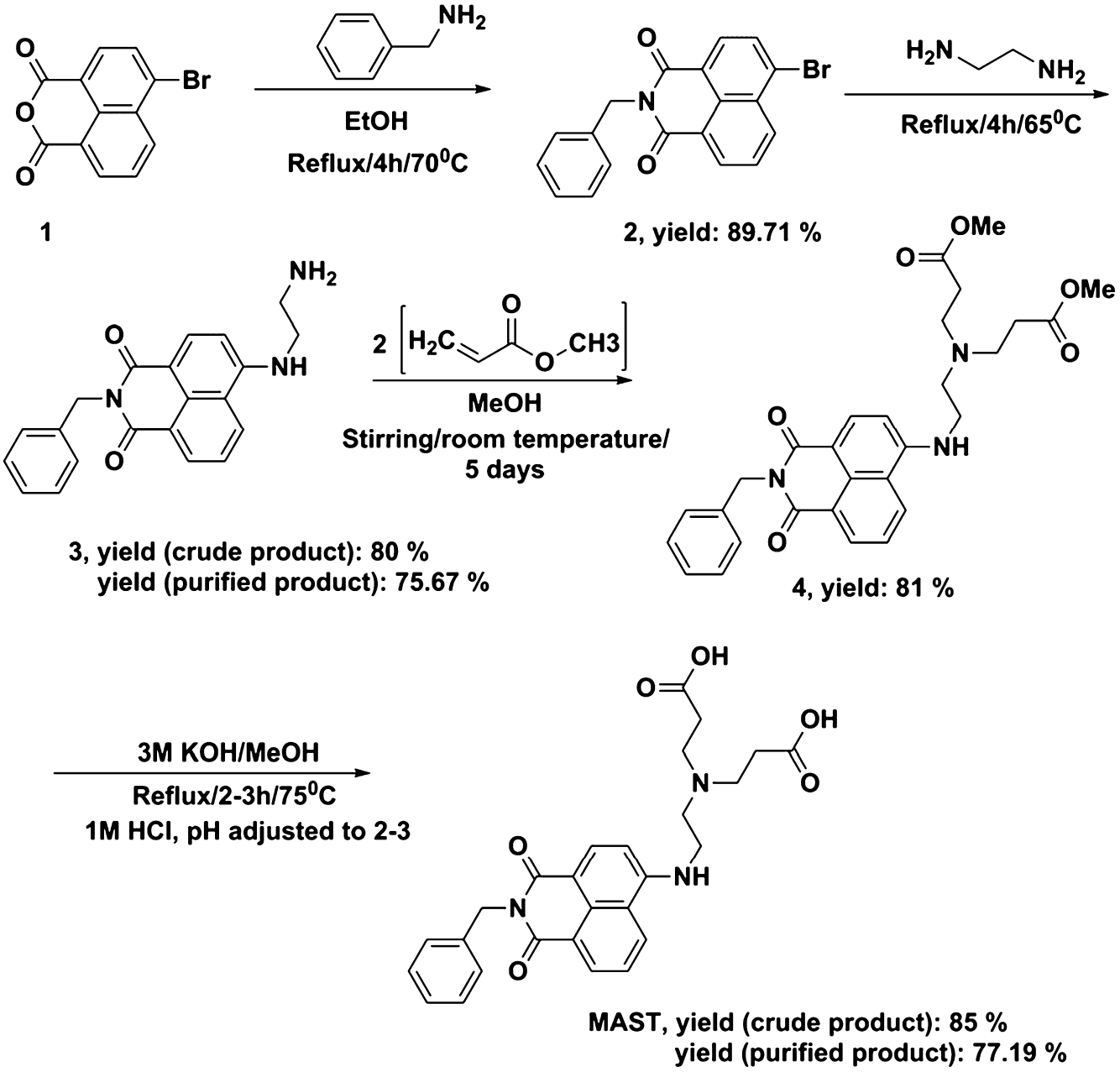

Scheme 1. The synthetic path to the chemosensor **MAST** and reference compounds **2** and **3**.

absorption band in the visible region, and large Stokes shifts.[28–37] Consequently, 1,8-naphthalimide derivatives have been found to be great applications for the generation of liquid crystal displays, laser active media, fluorescent markers in biology, photo-induced electron transfer (PET) chemosensors, electroluminescent materials, and fluorescence switches and chemosensors.[38–42]

To date, researchers from across the globe have performed well with regard to the design and synthesis of Cu^{2+}-selective fluorescence "turn off" chemosensors, with some of those findings referenced,[43–52] yet there are many milestones uncovered in the science of the design and development of Cu^{2+}-selective chemosensors.

In this present communication, the synthesis of a new variant of 1,8-naphthalimide that serves as a fluorescence "turn off" chemosensor for the selective detection of Cu^{2+}, which employs the "fluorophore-spacer-receptor" convention, based on the PET

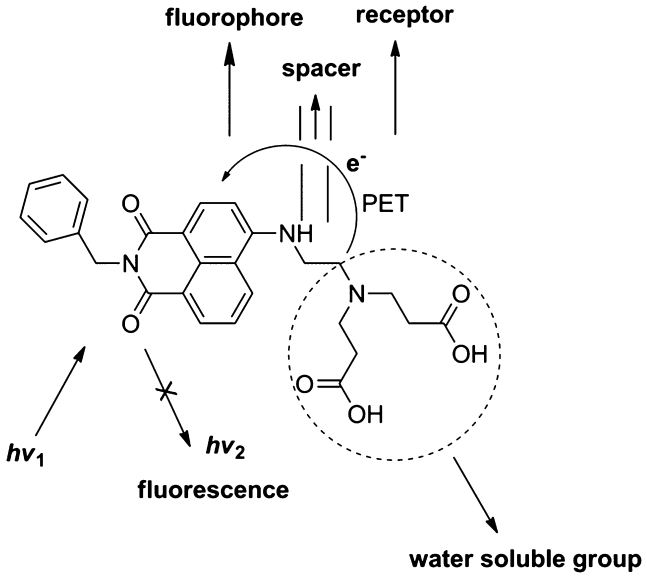

Scheme 2. The structure of the chemosensor **MAST**, showing the photo-induced electron transfer (PET) model employed for its design and the water-soluble carboxylic acid functional group.

mechanism, is being reported.[53] Interestingly, the chemosensor, which shows a significant solubility in an aqueous environment, also displays an ardent sensing property toward Cu^{2+} amidst the other metal ions tested and can be used for the monitoring of Cu^{2+} in the actual environmental system, specifically in water samples.

RESULTS AND DISCUSSION

Synthesis and characterization

The design concept of the chemosensor **MAST** stems from the "fluorophore-spacer-receptor" paradigm with a PET mechanism.[53] The route to the synthesis of the chemosensor **MAST** comprises a few steps, as explicitly illustrated in Scheme 1. 4-Bromo-1,8-naphthalic anhydride was utilized as the initiating material. Intermediate compounds **2** and **3** were obtained in accordance with the procedural steps reported by Misra *et al.*[1] The condensation of 4-bromo-1,8-naphthalic anhydride was achieved using 1-phenylmethanamine in an ethanol (EtOH) solvent to afford the intermediate compound **2**, which then underwent a nucleophilic aromatic substitution reaction upon the addition of ethylenediamine to give the intermediate compound **3**. The Michael addition reaction of the intermediate compound **3** with methyl acrylate in a methanol (MeOH) solvent yielded the intermediate compound **4**. Lastly, the desired chemosensor **MAST** was afforded in quantitative yield by undergoing acid hydrolysis. The full characterization of the chemosensor was performed by Fourier transform infrared red (FT-IR), ultraviolet–visible (UV–vis), proton nuclear magnetic resonance (^{1}H NMR) and carbon-13 nuclear magnetic resonance (^{13}C NMR) spectroscopic methods and MALDI-HRMS spectrometry (Figures S1–S4, Supporting information). All the data obtained were in good consistency with the structure of the proposed chemosensor.

In an attempt to come up with a chemosensor with an excellent solubility property, the carboxylic acid group has been incorporated into the receptor moiety of the newly derived compound, **MAST**, which is currently being reported. The choice of the carboxylic acid functional group owes its stimulation and reason to the fact that the –COOH group readily displays a great solubility in water. As such, while the chemosensor **MAST** was being designed, the author speculated that the incorporation of carboxylic acid groups into the architectural framework of the chemosensor would lead to its absolute solubility in an aqueous medium, which is a very desirable quality many spectroscopic chemosensors lack to date. Upon testing the solubility

Table 1. Photophysical properties of the chemosensor **MAST** (1 mM) in polar solvents buffered with HEPES (pH = 7.4)

Solvent	λ_F (nm)	λ_A (nm)	$\varepsilon_{max,}$ 10^4 (L/mol cm)	υ_A–υ_F (/cm)	Φ_F
DMSO	532	444	3.905	3580.1	0.11
DMF	523	440	7.530	3387.9	0.18
THF	506	429	5.183	3562.5	0.86
EtOH	527	443	2.637	3705.0	0.30
MeOH	528	440	4.650	4317.1	0.40
$(CH_3)_2CO$	516	429	4.087	4429.7	0.49
CH_3CN	517	430	3.751	3752.3	0.64

N = 3, RSD = 1.8%, where N = number of replicate determinations and RSD = relative standard deviation.

property of the obtained compound, it was soluble in water to a significant extent, even though not absolutely. **MAST** also displays complete and remarkable solubilities in dimethylsulfoxide (DMSO), dimethylformamide (DMF), tetrahydrofuran (THF), EtOH, MeOH, acetone $(CH_3)_2CO$, and acetonitrile (CH_3CN) but total insolubility in dichloromethane and tetrachloromethane. While Scheme 1 outlines the synthesis of chemosensor **MAST**, Scheme 2 summarizes the design module used for its obtainment.

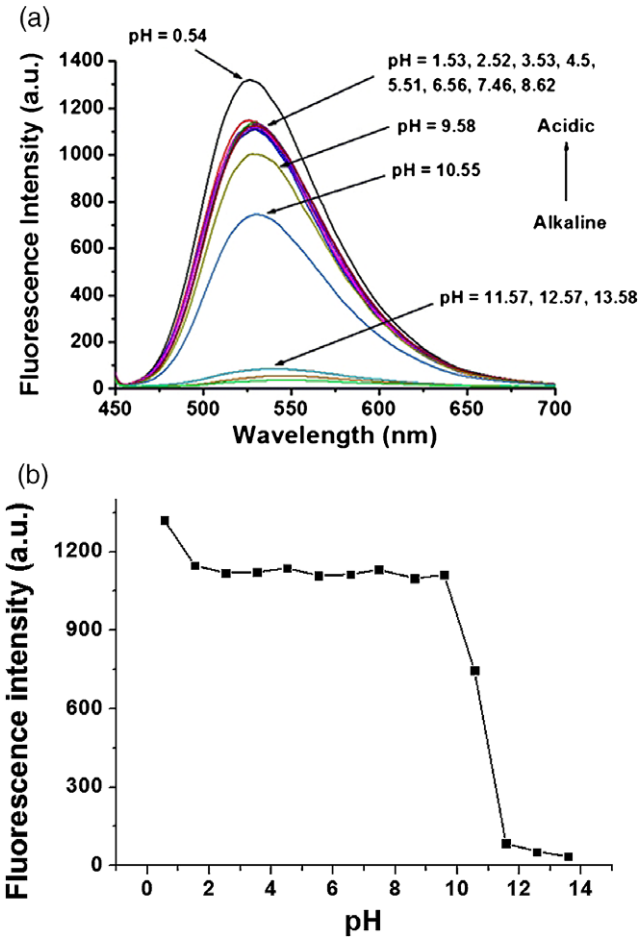

Fig. 1. (a) pH effect on the fluorescence spectra of the chemosensor **MAST** (0.1 mM) in HEPES-buffered DMSO solution; the pH was modulated by adding 1 M HCl and/or 1 M NaOH in double-distilled water. (b) The alterations at 529 nm with differing, increasing pH values. (*Note*: Three sets of parallel experiments were carried out, and the approximate errors were estimated to be about 3%).

Investigation of the photophysical properties of chemosensor MAST

The fact that 1,8-naphthalimide derivatives owe their absorption and fluorescence characteristics to the nature of the C-4 substituents on their rings is well established.[54,55] Table 1 presents the fundamental photophysical characteristics (absorption maxima, λ_A; fluorescence maxima, λ_F; molar extinction coefficient, ε_{max}; Stokes shift, υ_A–υ_F; and quantum fluorescence yield, Φ_F) of chemosensor **MAST** obtained in seven solvents of varying polarities. The solvents used for the assessment of the photophysical properties of chemosensor MAST were: DMSO, DMF, THF, EtOH, MeOH, $(CH_3)_2CO$, and CH_3CN. The photophysical studies were conducted in these solvents as they provide excellent solubilities for the chemosensor.

Notably, derivatives of 4-alkylamino-1,8-naphthalimide are strong, yellow-greenish, fluorescence-emitting fluorophores with maximal absorption bands of about 430–440 nm in the blue region, which are attributable to π–π* transitions. Under the naked eye, chemosensor **MAST** displayed a yellow color in each of these solvents, while it emitted a strong greenish fluorescence under UV light. The obtained fluorescence and absorption bands were in the regions of 506–532 and 429–444 nm, respectively.

Increasing the solvent polarity usually leads to a bathochromic shift of the maximum wavelength band. It is, therefore, expected that DMSO, which has the highest polarity, will display the highest values of the absorption and fluorescence wavelengths (i.e. λ_A and λ_F) and that THF, with the lowest polarity, will yield the lowest values of λ_A and λ_F. As speculated, these results were obtained and strongly correlated with the order of polarity. The range of the values of the molar extinction coefficient obtained is 26 370–75 300 L/mol cm, which is representative of the usually high molar extinction coefficients of typical 1,8-naphthalimide derivatives.

Stokes shift is a crucial photophysical parameter of fluorescent compounds that conveys the variations in the properties and structure of the fluorophores as they switch between the ground state S_0 and the first excited state S_1.[56] Based on the equation below,[57] the parameters of the Stokes shift (cm^{-1}) fell within the range of 3387.9–4429.7 cm^{-1}, which is in concordance with the data obtained for other blue-emitting 1,8-naphthalimide derivatives[58]:

$$(\nu_A - \nu_F) = \left(\frac{\lambda_F - \lambda_A}{\lambda_A \lambda_F}\right) \times 10^7 \quad (1)$$

The chemosensor **MAST** has large Stokes shift values that are beneficial as the excited and emitted radiation can be separated with more efficiency. Moreover, this attests to the well-established fact that Stokes shift is usually high in polar solvents, in which there is the favorable formation of hydrogen bond and dipole interactions, than in nonpolar solvents, in which there is not.[59] All the solvents used in this investigation are polar, and the values of the Stokes shifts obtained from them are commendable.

The fluorescence quantum yield (Φ_F) quantifiably typifies and signifies the potency of molecules to emit absorbed light and is determined using the equation below,[60] with *N*-butyl-4-*n*-butylamino-naphthalimide (Φ_F = 0.81 in EtOH) used as the standard:

$$\phi_F = \phi_r \frac{S_s A_r n_s^2}{S_r A_s n_r^2} \quad (2)$$

where Φ_F stands for the sample's emission quantum yield; Φ_r denotes the standard's emission quantum yield; A_r and A_s are the standard's and sample's absorbances at their respective excitation wavelengths; S_r and S_s connote the standard's and sample's integrated emission band areas, respectively; and n_r and n_s represent the standard's and sample's solvent refractive index, respectively.

The quantum yield decreases with increasing solvent polarity, with THF having the highest value and DMSO having the lowest. This is attributable principally to the PET quenching phenomenon. i.e. is usually observed in nonpolar media, which successively ensued in the regeneration of the fluorescence emission, and the PET processes that are accelerated in polar solvents.[61]

Investigation of the effect of pH on the sensing properties of chemosensor MAST

The next logical step would be to gain an understanding of the influence of operating pH on the sensing properties of chemosensor **MAST**. This will, in turn, inform the determination of the pH at which the proposed chemosensor performs best, which will largely influence the sensing characteristics of the chemosensor. It is generally known that the presence or absence of protons in the vicinities of fluorescent chemosensors induces an influence on their sensing behaviors, which in turn affect their sensitivities in the detection of an analyte.

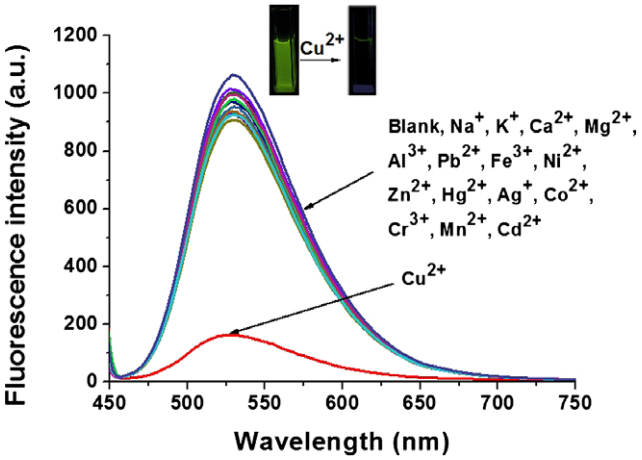

Fig. 2. Fluorescence response of chemosensor **MAST** (0.1 mM) to Cu^{2+} (0.1 mM) or to a mixture of each of the specified metal ions (0.1 mM) with Cu^{2+} (0.1 mM) in HEPES-buffered DMSO solution (v/v, 1:1; pH 7.4). (*Note*: Three sets of parallel experiments were carried out, and the approximate errors were estimated to be about 2.5%).

With this in mind, the fluorescence spectra of the chemosensor **MAST** was monitored as a function of variation in pH by conducting pH titration of the chemosensor **MAST** with solutions of different pH values. To acquire a great depth of insight, a wide pH range of 0.54–13.58 was utilized, with the pH modulated incrementally with 1 M HCl and/or 1 M NaOH, starting from the acidic region. As shown in Figure 1(a), upon acidification, large fluorescence enhancements were observed in the starting pH range of 0.54–1.53, with the implication that the fluorescence emission is highly dependent on the pH in the acidic region. This is accrued to the protonation of the aniline nitrogen on the naphthalimide ring,[3] which in turn weakened its interaction with Cu^{2+}, thereby leading to enhanced fluorescence intensity ("turned on" fluorescence). More interestingly, only minuscule changes (less than 2.46% variation) in the fluorescence intensity of the chemosensor occurred in the pH region 1.53–8.62. Simply put, the determination of Cu^{2+} with the chemosensor **MAST** was not significantly affected by variation in pH in this region. This is, therefore, proof that the synthesized

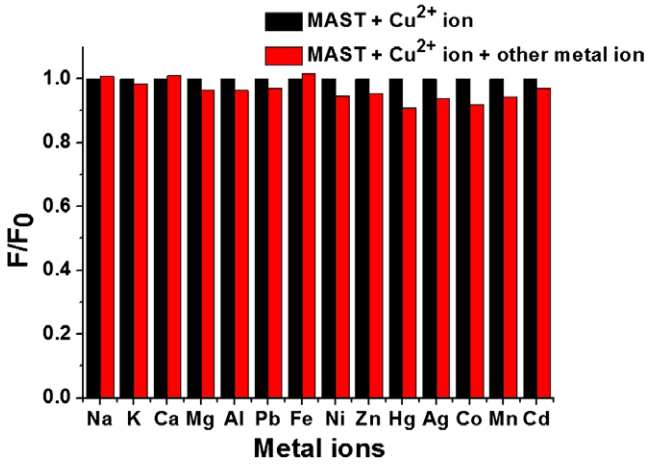

Fig. 3. Fluorescence spectra of the chemosensor **MAST** (0.1 mM) in HEPES-buffered DMSO solution (v/v, 1:1; pH 7.4) in the joint existence of differing quantities of competing metal ions (0.1 mM). (*Note*: Three sets of parallel experiments were carried out, and the approximate errors were estimated to be about 2.7%).

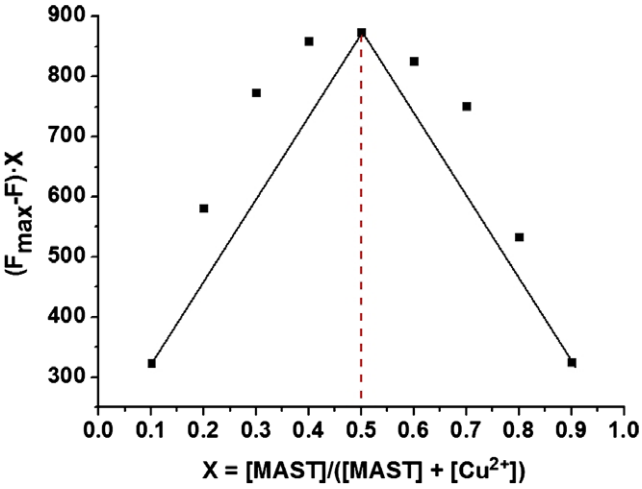

Fig. 4. Job plot for the complex [Cu(**MAST**)] (the entire concentration of **MAST** and Cu^{2+} was held constant at 100 μM). (*Note*: Three sets of parallel experiments were performed, and the approximate errors were estimated to be approximately 4.6%).

chemosensor could facilitate the monitoring of Cu^{2+} in a wide pH span, and can behave as a functional chemosensor in low- and medium-pH value media. Based on experimental results as justified in Figure 1(b), pH 7.4 was chosen as the optimum pH value at which the proposed chemosensor works best under experimental conditions.

Conversely, the fluorescence intensity of the chemosensor suffered a marked decrease ("turned off" fluorescence) in the pH region 9.58–13.58. This is attributed to the deprotonation of the hydroxyl functional group in the receptor moiety, which in turn led to an extension of the conjugation, and thereby reduced the fluorescence intensity.

Spectroscopic assessment of chemosensor MAST in the presence of various metal ions

The fluorescence response of the chemosensor **MAST** to various metal ions, i.e. Na^{+}, K^{+}, Ca^{2+}, Mg^{2+}, Al^{3+}, Pb^{2+}, Fe^{3+}, Ni^{2+}, Zn^{2+}, Hg^{+}, Ag^{+}, Co^{2+}, Cr^{2+}, Mn^{2+}, Cd^{2+}, and Cu^{2+} in HEPES-buffered DMSO solution (v/v, 1:1; pH 7.4) under excitation at 435 nm was investigated. In the absence of the metal ions, the chemosensor exhibited large fluorescence strength (an intensive greenish fluorescence) at 529 nm. As Figure 2 clearly depicts, when each of the metal ions was introduced into a 0.1 mM HEPES-buffered DMSO solution (v/v, 1:1; pH 7.4), only Cu^{2+} was able to quench the fluorescence of the chemosensor. This spectacular observation occurred instantly, affording an 83.67% fluorescence decrease or 6.12-fold fluorescence quenching (Φ_F = 0.018). This observation is ascribable to the coordination of the powerful paramagnetic Cu^{2+} to the receptor unit of the chemosensor, which effected a fluorescence "turn off" behavior when the solution of each of the metal ions was added.[48–52] In sharp contrast, each of the other metal ions investigated under the same conditions had a collective benign effect (a persistent greenish color under UV light) on the fluorescence intensity of the chemosensor. These outcomes clearly furnish the evidence that the chemosensor **MAST** exhibits both singular and ardent signaling behavior toward Cu^{2+} and could effectively discriminate Cu^{2+} in an admixture of several other metal ions. Moreover, this commendable result validates the soundness of our design strategy of the chemosensor **MAST**.

Selectivity study of MAST for Cu^{2+} over competitive metal ions

Whether a proposed compound will act as an ideal chemosensor or not is largely a matter of its selectivity. As such, the selectivity property of the proposed chemosensor was studied by looking at the effects of other metal ions on its sensing properties. Drawing on this,

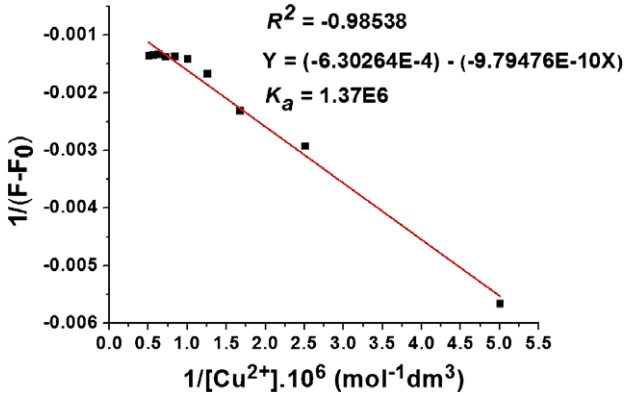

Fig. 5. Benesi–Hildebrand plot for the estimation of the association constant of complex [Cu(**MAST**)], using a 1:1 stoichiometry for the interaction between **MAST** and Cu^{2+}. (*Note*: Three sets of parallel experiments were carried out, and the approximate errors were up to 4%).

fluorescence competitive experiments were conducted in the presence of Cu^{2+} at a concentration of 0.1 mM mixed with each of the various interfering metal ions, specifically Na^{+}, K^{+}, Ca^{2+}, Mg^{2+}, Al^{3+}, Pb^{2+}, Fe^{3+}, Ni^{2+}, Zn^{2+}, Hg^{+}, Ag^{+}, Co^{2+}, Cr^{2+}, Mn^{2+}, Cd^{2+}, and Cu^{2+}, which were also at concentrations of 0.1 mM. Figure 3 demonstrates the plot of the ratios of the fluorescence intensities versus the wavelength and vividly indicates that the competition between Cu^{2+} and other metal ions for the dampening of the fluorescence chemosensor **MAST** is modest. Meanwhile, Cu^{2+} is the only ion that significantly suppressed the fluorescence intensity of the chemosensor **MAST**. Likewise, the emission color is independent of the metal ion added, except for Cu^{2+} ion, which induced a near-colorless effect on the solution of the chemosensor. In short, the addition of each of the metal ions does not impose a prominent disturbance on the fluorescence of the [Cu(**MAST**)] complex. These results strongly correlated with those acquired in the previous section. This clearly demonstrates that the selectivity of the proposed chemosensor is excellently high and that the chemosensor could retain its sensing properties toward Cu^{2+} under the potential competition of other metal ions. This is a further attestation to the soundness of the proper choice of entities used in the construction of the chemosensor **MAST**.

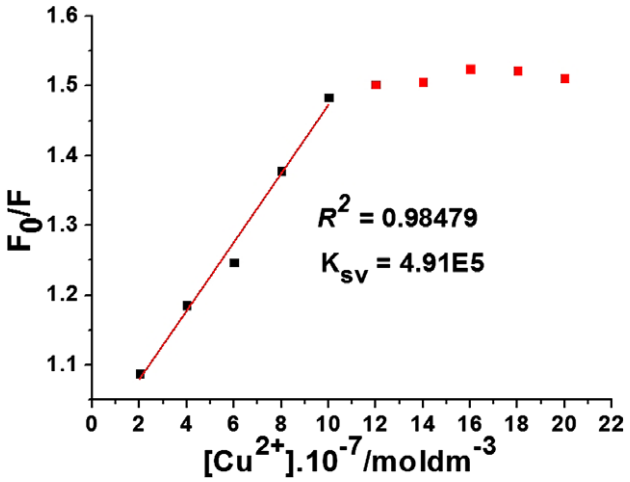

Fig. 6. The Stern–Volmer plot of the ratio of the fluorescence intensities F_0/F (where F_0 is the blank's fluorescence intensity, which is 2191) of the chemosensor **MAST** against the increasing concentration of Cu^{2+} ([Cu^{2+}] = 10–100 μM). (*Note*: Three sets of parallel experiments were carried out, and the approximate errors were estimated to be about 3%).

Determination of the stoichiometric ratio and binding constant

The method of continuous variation, i.e. Job plot,[62] was used to obtain the coordination stoichiometry of the complex formed, [Cu(**MAST**)], between the chemosensor **MAST** and Cu^{2+}. The maxima at the mole fraction at 0.5 of the Job plot (Figure 4) clearly reveals the formation of a 1:1 complex between the chemosensor **MAST** and Cu^{2+} ion.

The association constant and detection limit (DL) of the chemosensor **MAST** were determined by employing the 1:1 stoichiometry. First, the association constant (K_a) of the chemosensor **MAST** was estimated using the Benesi–Hildebrand equation[63]:

$$\frac{1}{F-F_0} = \frac{1}{K_a\,(F_{\min}-F_0)\,[Cu^{2+}]^n} + \frac{1}{F_{\min}-F_0} \qquad (3)$$

where F is the fluorescence intensity at 529 nm at any given concentration of Cu^{2+}, F_0 is the fluorescence intensity at 529 nm in the absence of Cu^{2+}, $F_{\min}$ is the minimum fluorescence intensity at 529 nm in the presence of Cu^{2+} in solution, and n is the stoichiometric mole ratio, which is 1 in this case. The association

constant was appraised by graphically plotting $1/(F - F_0)$ against $1/[Cu^{2+}]$ (Figure 5). Data were subjected to linear fits according to the above equation, and the K_a value was determined from the line's slope. The value of the association constant was calculated to be 1.37 ($\pm$0.04) $\times$ 10^6 M^{-1} (the calculated percentage errors were less than 3%), which is large enough and indicates an intense binding of the chemosensor **MAST** with the Cu^{2+} ion. This value correlates with those obtained for other Cu^{2+} chemosensors.[64–67]

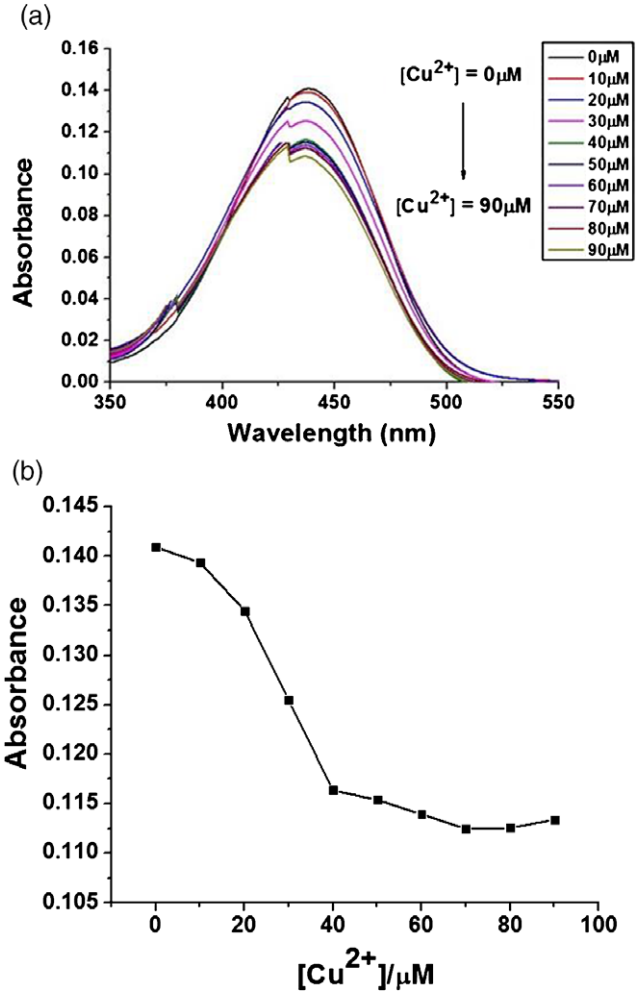

Fig. 7. (a) Absorption spectra response of **MAST** (0.1 mM) in HEPES-buffered DMSO solution (v/v, 1:1; pH 7.4) upon the addition of different concentrations of Cu^{2+} (0.04 mM). (b) Changes in absorbance at 438 nm with differing, increasing Cu^{2+} concentrations. (*Note*: Three sets of parallel experiments were carried out, and the approximate errors were estimated to be about 3%).

Determination of DL of chemosensor MAST

The fluorescence quenching for the "turn off" phenomenon was evaluated quantitatively by observing the Stern–Volmer plot of the ratio of the fluorescence intensities versus the concentration of Cu^{2+} (Figure 6) based on the equation below[68]:

$$\frac{F_0}{F} = 1 + K_{sv}[Q] \quad (4)$$

where F_0 is the initial fluorescence intensity; F is the fluorescence intensity measured in the presence of the analyte; $[Q]$ is the concentration of the quencher, which is $[Cu^{2+}]$ in this case; and K_{sv} is the Stern–Volmer constant. When (F_0/F) is plotted against $[Q]$, the plot was a straight line graph, with K_{sv} being equivalent to the value of the slope.

The *DL*,[69] which is also a distinctive feature any proposed compound must possess to qualify as an ideal chemosensor, was equally obtained. The *DL* of chemosensor **MAST** toward Cu^{2+} was calculated based on the equation below:

$$DL = \frac{3\sigma}{K_{sv}} \quad (5)$$

where σ is the blank solution's standard deviation, and K_{sv} is the calibration plot's slope. *DL* was calculated to be 0.69 ($\pm$0.03) $\times$ 10^{-8} M (the calculated percentage errors were about 3%), which is far lower than the WHO and US EPA regulated limits of 31.5×10^{-6} and 20×10^{-6} M, respectively,[14,23] for Cu^{2+} in drinking water. This result substantiates that the proposed chemosensor **MAST** has the potency to monitor Cu^{2+} in acceptably low concentrations whether in the environmental or biological system.

All the experiments above yielded robust results, and the aforementioned findings fit exactly with the focus of this present communication—the synthesis of a Cu^{2+}-selective fluorescence "turn off" chemosensor. It can, therefore, be argued that the proposed chemosensor **MAST** meets the criteria for the highly selective Cu^{2+} sensing in a competitive medium of various physiologically and environmentally relevant metal ions.

UV–Vis and fluorescence titration of chemosensor MAST toward Cu^{2+}

To investigate the binding affinity of the chemosensor **MAST** with Cu^{2+}, UV–vis and fluorescence

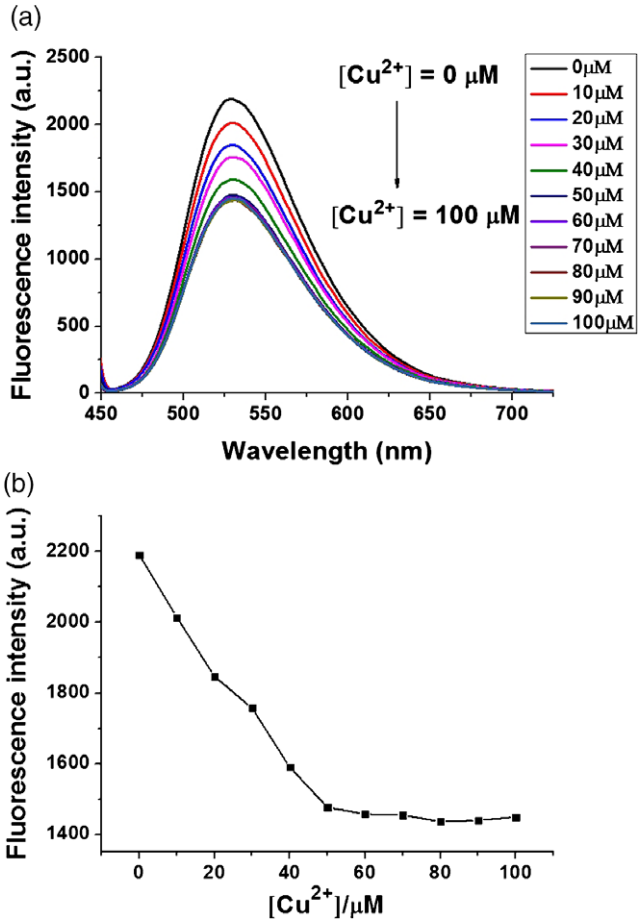

Fig. 8. (a) Changes in the fluorescent spectra of the chemosensor **MAST** (0.1 mM) in HEPES-buffered DMSO solution (v/v, 1:1; pH 7.4) upon the addition of different Cu^{2+} concentrations (0.04 mM). (b) The changes in the fluorescence intensity at 529 nm with differing, increasing Cu^{2+} concentrations (excitation was performed at 435 nm). (*Note*: Three sets of parallel experiments were carried out, and the approximate errors were estimated to be about 3.1%).

titration experiments were conducted. The spectral behavior of the chemosensor **MAST** (0.1 mM) in HEPES-buffered DMSO solution (v/v, 1:1; pH 7.4) was recorded. The uncomplexed chemosensor displayed a profound absorption band centered at λ_{max} = 438 nm (ε_{max} = 1.4093 × 10^5 L/mol cm), which is responsible for its sharp yellow color in solution. The chemosensor also emits an intensive greenish fluorescence at λ_F = 529 nm (Φ = 0.107), which is a representative feature of the fluorescence quantum yields of some fluorescent and 4-amino-1,8-naphthalimide compounds.[70–73] The

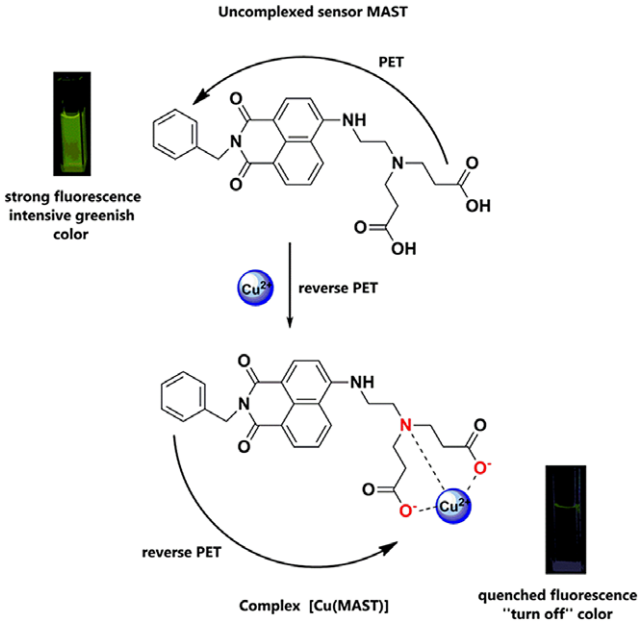

Scheme 3. The proposed binding mode of the chemosensor **MAST** with Cu^{2+}. The strong greenish fluorescence was turned off by Cu^{2+} in HEPES-buffered DMSO solution (v/v, 1:1; pH 7.4). Inset: the initially strong and consequently dampened fluorescence emission colors of the designated compound **MAST**.

details of the titration studies conducted are given below.

UV–vis titration studies Figure 7(a) provides the UV–vis absorption titration profile of the chemosensor **MAST** with varying concentrations of Cu^{2+} solution. When the concentration of Cu^{2+} was increased (the increment was by a factor of 10, starting from 10 up to 100 μM), the intensity of the main absorption peak at 438 nm underwent an apparent gradual decrease, followed by the concomitant formation of a new signal band positioned at 437 nm until a well-defined isosbestic point at 429 nm was formed. Moreover, the dose-dependent absorbance quenching of the chemosensor toward Cu^{2+}, as demonstrated in Figure 7(b), exhibited a good linearity even up to when 50 μM of the Cu^{2+} solution was added.

Fluorescence titration studies Utilizing experimental procedures similar to those of UV–vis titration, further insights into the sensing properties of the chemosensor **MAST** were obtained by investigating the fluorescence titration reaction curve of the changes in the

fluorescence spectra of the chemosensor toward varying amounts of Cu^{2+} (Figure 8(a)). The fluorescence titration of the chemosensor **MAST** with Cu^{2+} experiment reveals that the fluorescence intensity of the chemosensor was quenched in a steady manner in response to the gradual increase in the concentrations of the added Cu^{2+} in HEPES buffered-DMSO solution (v/v, 1:1; pH 7.4), with a bathochromism of about 3 nm observed. This could be explained on the basis of the complexation of Cu^{2+}, which lowers the electron-releasing potency of the nitrogen atom in the receptor moiety,[74] thereby inhibiting the PET mechanism and the paramagnetic property of Cu^{2+}. This observed phenomenon of fluorescence quenching indicates that the chemosensor can effectively act as a "turn off" chemosensor toward Cu^{2+}. As clearly depicted in Figure 8(b), the dose-dependent fluorescence quenching of the chemosensor toward Cu^{2+} showed a good linearity even up to when 50 μM of the Cu^{2+} solution was added so that 50 μM could be set as the threshold for the determination of Cu^{2+}. This is an encouraging outcome, which establishes the effectiveness of the proposed chemosensor to detect quantitatively relevant concentrations of Cu^{2+}.

Proposed sensing mechanism

The chemosensor **MAST** was designed as a typical example of PET sensors that exploit the general fluorophore-spacer-receptor format.[53] Scheme 3 provides a detailed schematic illustration of the proposed binding mode. The binding mode of the chemosensor **MAST** toward the Cu^{2+} ion, which resulted in a remarkable dampening of the intensity of the fluorescence spectrum, is due to two plausible reasons. On the one hand, when a fluorescence group is joined to an electron-donating group (in this case, the amido nitrogen atom), there is a transduction of the PET effect between the fluorescence moiety and the electron donation unit.[75] In the chemosensor **MAST**, an aliphatic secondary amine connects to the naphthalimide fluorophore. In an alkaline medium, an aliphatic amine usually acts as a powerful electron-releasing group. Under this condition, the intensity of the fluorescence of the chemosensor **MAST** exists in the "off state" due to the quenching of the intensity of the fluorescence of the naphthalimide fluorophore by the PET process. On the other hand, the binding mode is also partly the result of the strong, intrinsic paramagnetic behavior of the Cu^{2+} ion.[48–52]

Real-world application of chemosensor MAST for Cu^{2+} quantification

The designated chemosensor **MAST** was used to determine the amounts of Cu^{2+} in real water samples. The water samples employed for the analysis were sourced from the famous Yellow River (Lanzhou city), while the tap water samples were acquired from our school. The samples were suitably spiked with the standard Cu^{2+} solutions at various levels of concentrations. Thereafter, they were analyzed with the chemosensor **MAST**. The measurements were performed at three ($N = 3$) replicate determinations for each of the Yellow River and tap water samples. As depicted in the table, the relative standard deviation (RSD) at the Cu^{2+} sample concentrations were determined to be sufficiently low (within the range of 0.02–0.30 μM). The recoveries of the spiked Cu^{2+} were calculated and summarized in Table 2. The results of the analysis demonstrated recoveries in the range of 98–109.80%, meaning that the chemosensor actually has potential for the detection of Cu^{2+} in actual samples.

Table 2. Results of the analysis of Cu^{2+} ion determination in different water samples using the proposed chemosensor **MAST**

Water sample	Cu^{2+} spiked (μM)	Cu^{2+} recovery, mean ± SD (μM)	Recovery (%)
Yellow	2	2.01 ± 0.11	101.00
River	3	3.12 ± 0.22	105.62
	4	3.96 ± 0.14	98.75
Tap	2	1.89 ± 0.02	98.00
	3	3.05 ± 0.23	103.30
	4	4.23 ± 0.30	109.80

$N = 3$, where N = number of replicate determinations.

EXPERIMENTAL

Reagents and materials

The grade of the solvents and reagents used for the syntheses were analytical reagent, and the materials were utilized just as bought without any further purification performed, except if stipulated. Twice-distilled water was used in all syntheses, while deionized water was used for all spectroscopic measurements. Sixteen nitrate and chloride metal salts were used as the sources of the metal ions. Specifically, they are $NaNO_3$, KNO_3, $CaCl_2$, $MgCl_2$, $Al(NO)_3$, $Pb(NO_3)_2$, $Fe(NO_3)_3$, $Ni(NO_3)_2$, $Zn(NO_3)_2$, $Cu(NO_3)_2$, $Hg(NO_3)_2$, $AgNO_3$, $Co(NO_3)_2$, $Cr(NO_3)_3$, $Mn(NO_3)_2$, and $Cd(NO_3)_2$. HEPES (pH = 7.4) was used as the buffer solution. All experiments were performed at room temperature.

Instrumentation

The progress of all reactions was periodically monitored by thin-layer chromatography (TLC) performed on silica gel, Fluka F60 254, 20 × 20, 0.2 mm (Merck KGaA, Germany). Melting points were determined with XD-4 digital micromelting point apparatus (Beijing, China) and were uncorrected. The Fourier transform infrared (FT-IR) spectra were recorded in the 4000–400 cm^{-1} region with a Varian Scimitar 1000 spectrometer (Madison, WI, USA) using KBr pellets. Electrospray ionization mass spectra (ESI-MS) were acquired using a BRUKER micrOTOF-Q system (Kontich, Belgium). UV–vis spectra were assessed using a LabTech BlueStar Plus UV–vis spectrophotometer (Tianjin, China). Fluorescence spectra were measured using a Lengguang Tech. F97 Pro spectrofluorometer (Shanghai, China). All the absorption and fluorescence spectra were recorded at 25°C in a 1 cm × 1 cm quartz cuvette (3 mL) utilizing a 10 nm bandwidth and a 3000 nm/min scan rate. The spectra of ^1H NMR and ^{13}C NMR were recorded on a Varian Mercury Plus 400 spectrometers (Palo Alto, CA, USA), with tetramethylsilane (TMS) as the internal standard and DMSO-d_6 as the solvent. Data, graphs, and chemical structures were analyzed, plotted, and drawn with Microsoft Excel, Origin 8.5, Mnova NMR, ChemDraw Ultra 12.0, and Omnic™ software. The pHs of the cation solutions used were adjusted using a Beckman Coulter F360 pH meter (Brea, CA, USA) utilizing M HCl and/or 1 M NaOH.

Procedures for spectroscopic measurements

The cations' stock solutions (1 mM) were prepared from the metal salts $NaNO_3$, KNO_3, $CaCl_2$, $MgCl_2$, $Al(NO)_3$, $Pb(NO_3)_2$, $Fe(NO_3)_3$, $Ni(NO_3)_2$, $Zn(NO_3)_2$, $Cu(NO_3)_2$, $Hg(NO_3)_2$, $AgNO_3$, $Co(NO_3)_2$, $Cr(NO_3)_3$, $Mn(NO_3)_2$, and $Cd(NO_3)_2$. Test solutions of the metal ions were prepared using double-distilled water by diluting the stock solutions to the desired molar concentration (0.1 mM). Similarly, the stock solution (1 mM) of the chemosensor **MAST** was prepared in the DMSO solvent, while the test solution of the chemosensor was obtained by diluting the stock solution to the desired molar concentration (0.1 mM). The absorption and fluorescence spectra of the solution of the chemosensor cation were recorded using the mixture of 2 mL of HEPES buffer solution, 20 μL of sample solution of the chemosensor, and 100 μL of each of the various metal ions in a 1 cm × 1 cm quartz cuvette. The mixture was allowed to stand for 1 min for thorough mixing. The fluorescence measurements were conducted at the 435 nm maximum excitation wavelength and the 750 nm maximum emission wavelength, while the absorbance measurements were carried out at the wavelength range of 180–550 nm. All the spectroscopic experiments were performed in triplicates (i.e. $N = 3$).

Synthesis of compounds

The proposed fluorescent chemosensor **MAST** was devised through a stepwise synthetic route of four steps as outlined in Scheme 1. The starting point of the synthesis was 4-bromo-1,8-naphthalic anhydride (compound **1**). Intermediate compounds **2** and **3** were synthesized by the slight modification of the procedures earlier reported by Misra *et al.*[1]

Synthesis of intermediate compound 2 The compound **1**,4-bromo-1,8-naphthalic anhydride (8.30 g, 0.03 mol) dissolved in 80 mL EtOH was added to 1-phenylmethanamine (5 mL, 0.05 mol) in 20 mL of EtOH. The resultant mixture was heated under reflux and stirred for 4 h at 70 °C. The progress of the reaction was monitored by TLC analysis using ethyl acetate/hexane (v/v, 2:8) as the eluent. After the complete reaction was ascertained, 250 mL of cold water was added to the reaction mixture to facilitate the precipitation of the desired product. The precipitated product was then isolated by vacuum filtration and washed with 10% aqueous Na_2CO_3 and distilled water. The product

was finally dried and obtained as an off-white solid; yield: 89.71%, M.p.: 140–142°C.

Synthesis of intermediate compound 3 The intermediate compound **2** (1.00 g, 0.0027 mol) was added to a solution of ethylenediamine (11.00 g, 0.183 mol) in a two-necked 500 mL, round-bottom flask, which was heated to a temperature of 65°C on a reflux apparatus. The resultant mixture was heated to reflux for 4 h with thorough stirring at 65 °C. TLC monitoring of the reaction was performed at an hourly interval using 2 mL of MeOH as the eluent. After the reaction was complete, the reaction mixture was cooled to room temperature; 100 mL of distilled water was then poured into the solution, whereupon the precipitate formed was collected by suction filtration, washed with distilled water, and dried under vacuum. The crude product was afforded in 80% yield. The purification of the crude product was performed by column chromatography on a silica gel stationary phase with MeOH as the eluent; yield: 75.67%; M.p.: 169–170°C.

Synthesis of intermediate compound 4 A solution of methyl acrylate (2.50 g, 0.029 mol) in 10 mL of MeOH was added slowly to a solution of intermediate compound **3** (1.00 g, 0.0029 mol) in 60 mL of MeOH via a syringe for a 30-min time frame. Thereafter, the reaction mixture was continuously stirred for a 5-day time frame at room temperature, the surplus methyl acrylate was collected by suction filtration, and the intermediate product **4** was afforded as a solid of yellow color and then dried under vacuum; yield: 81%; M.p.: 178–179°C.

Synthesis and characterization of the proposed chemosensor N-phenyl-4-(3,3′-((2-aminoethyl)azanediyl)dipropanoic acid)-1,8-naphthalimide (MAST) The desired compound **MAST** was obtained in a quantitative yield by the hydrolysis of intermediate compound **4** with potassium hydroxide in MeOH solvent under reflux conditions for 2–3 h at a temperature of 75°C, followed by acidification by the drop-wise addition of 1 M HCl solution until the pH reached 2–3. Once this pH range was reached, a red precipitate of the desired product was formed, which was then collected by vacuum filtration and washed thoroughly with water; yield: 85%; M.p.: 170–174°C. The crude product was finally recrystallized in EtOH to afford the pure product; yield: 77.19%; M. p.: 167–168°C. MS (ES^+) m/z = 490.1853 $(M + H)^+$. FT-IR (ν_{max}, KBr, cm^{-1}): 757 (ν_{Ar}); 3381 (νNH); 2603 and 2592 (νN); 2871 and 2960 (νCH); 1684 (ν^{as}N—*C*═*O*); 1646 (ν^{s}N—*C*═*O*); 1717 (νC═O of COOH); 3663 and 3669 (νOH of COOH); 1550 and 1582 (νC═C, aromatic); 1300 and 1350 (νC—O of COOH). UV–vis (in DMSO, nm): 259, 445. ^{1}H NMR (300 MHz, DMSO-d_6): δ = 8.57 (d, 1H, J = 7.3 Hz, naphthalimide H-5); 8.45 (d, ^{1}H, J = 8.6 Hz, naphthalimide H-2); 8.38 (dd, 1H, J = 8.3 Hz, J = 1.0 Hz, naphthalimide H-7); 7.60 (dd, ^{1}H, J = 8.3 Hz, J = 7.3 Hz, naphthalimide H-6); 6.67 (d, ^{1}H = 8.6 Hz, naphthalimide H-3); 6.28 (m, ^{1}H, NH); 4.16 (t, 2H, J = 7.6 Hz, $(CO)_2NCH_2$); 11.0 (s, 2H, 2 × OH); 2.39 (t, 4H, J = 6.4 Hz, 2 × CH_2COOH); 7.54 (d, 2H, J = 7.2 Hz, benzene), 7.25 (m, 3H, benzene). ^{13}C NMR (400 MHz, DMSO-d_6): 176.64, 175.04, 168.80, 167.97, 154.96, 143.02, 139.20, 135.97, 134.24, 133.40, 132.73, 132.04, 129.58, 126.67, 125.47, 113.68, 109.38, 65.72, 56.02, 53.31, 53.14–52.66, 47.65, 45.31, 45.13, 44.71, 44.55–44.53, 44.40, 44.22, 44.09, 42.74, 33.44, 19.07.

CONCLUSIONS

In summary, we have successfully constructed a new, highly potent 1,8-naphthalimide-based fluorescence "turn off" chemosensor, **MAST** and evaluated its sensing properties toward Cu^{2+}. The compound yielded a significant solubility in water and in a host of other solvents. Through a dampened fluorescence mechanism, the chemosensor upheld a strict monopoly for the sensing of Cu^{2+} in HEPES-buffered DMSO solution (v/v, 1:1; pH 7.4) in the presence of the other competitive metal ions, such as Na^+, K^+, Ca^{2+}, Mg^{2+}, Al^{3+}, Pb^{2+}, Fe^{3+}, Ni^{2+}, Zn^{2+}, Hg^+, Ag^+, Co^{2+}, Cr^{2+}, Mn^{2+}, Cd^{2+}, and Cu^{2+}. The DL of the chemosensor for the monitoring of Cu^{2+} reached the level of 1.69×10^{-8} M, which was lower than the WHO and US EPA limits of 31.5 and 20 μM, respectively, thereby opening up inspiration for the definitive role of the chemosensor for the practical quantitative analysis of Cu^{2+}.

It is apparent that the proposed chemosensor fits the description of an excellent example of Cu^{2+}-selective fluorescence "turn off" chemosensors. Presently, the research team to which the author belongs is actively working on the generation of newer architectures of 1,8-naphthalimide-based fluorescent chemosensors for other ions. With devoted efforts, I look forward to reporting the future research investigations in due course.

ACKNOWLEDGMENT

This work was supported by the China Scholarship Council under the CSC No. 2014BSZ528.

SUPPORTING INFORMATION

Additional supporting information is available in the online version of this article.

REFERENCES

1. A. Misra, M. Shahid, P. Srivastava, *Sens. Actuators B: Chem.* **2012**, *169*, 327.
2. V. B. Bojinov, I. P. Panova, D. B. Simeonov, N. I. Georgiev, *J. Photochem. Photobiol. A: Chem* **2010**, *210*, 89.
3. Q. Li, Y. Guo, S. J. Shao, *Sens. Actuators B: Chem.* **2012**, *872*, 171.
4. G. Aragay, J. Pons, A. Merkoci, *Chem. Rev.* **2011**, *111*, 3433.
5. D. T. Quang, J. S. Kim, *Chem. Rev.* **2010**, *110*, 6280.
6. N. Kaur, S. Kumar, *Tetrahedron* **2011**, *67*, 9233.
7. G. C. Kuang, J. R. Allen, M. A. Baird, B. T. Nguyen, L. Zhang, T. J. Morgan Jr, C. W. Levenson, M. W. Davidson, L. Zhu, *Inorg. Chem.* **2011**, *50*, 10493.
8. M. Dutta, D. Das, *Trends Anal. Chem.* **2012**, *32*, 113.
9. H. N. Kim, W. X. Ren, J. S. Kim, J. Yoon, *Chem. Soc. Rev.* **2012**, *41*, 3210.
10. A. Barba-Bon, A. M. Costero, S. Gil, M. Parra, J. Soto, R. Martínez-Máñez, F. Sancenón, *Chem. Commun.* **2012**, *48*, 3000.
11. E. L. Que, D. W. Domaille, C. J. Chang, *Chem. Rev.* **2008**, *108*, 1517.
12. B. Valeur, I. Leray, *Coord. Chem. Rev.* **2000**, *205*, 3.
13. J. Cho, T. Pradhan, Y. M. Lee, J. S. Kim, S. Kim, *Dalton Trans.* **2014**, *43*, 16178.
14. G. R. You, G. J. Park, J. J. Le, C. Kim, *Dalton Trans.* **2015**, *44*, 9120.
15. H. Tapiero, D. M. Townsend, T. D. Tew, *Biomed. Pharmacother.* **2003**, *57*, 386.
16. K. J. Barnham, C. L. Masters, A. I. Bush, *Nat. Rev. Drug Discov.* **2004**, *3*, 205.
17. S. Mare, S. Penugonda, S. M. Robinson, S. Dohgu, W. A. Banks, N. Ercal, *Peptides* **2007**, *28*, 1424.
18. B. E. Kim, T. Nevitt, D. J. Thiele, *Nat. Chem. Biol.* **2008**, *4*, 176.
19. J. C. Lee, H. B. Gray, J. R. Winkler, *J. Am. Chem. Soc.* **2008**, *130*, 6898.
20. A. Mokhir, A. Kiel, D. P. Herten, R. Kraemer, *Inorg. Chem.* **2005**, *44*, 5661.
21. J. Liu, *J. Am. Chem. Soc.* **2007**, *129*, 9838.
22. R. A. Løvstad, *Biometals* **2004**, *17*, 111.
23. H. S. Jung, P. S. Kwon, J. W. Lee, J. Kim II. , C. S. Hong, J. W. Kim, S. H. Yan, J. Y. Lee, J. H. Lee, T. H. Joo, J. S. Kim, *J. Am. Chem. Soc.* **2009**, *131*, 2008.
24. J. Kumar, P. K. Bhattacharyya, D. K. Das, *Spectrochim. Acta A.: Mol. Bimol. Spect.* **2015**, *138*, 99.
25. K. Aggarwal, J. M. Khurana, *J. Lumin.* **2015**, *167*, 146.
26. M. Royzen, Z. H. Dai, J. W. Canary, *J. Am. Chem. Soc.* **2005**, *127*, 1612.
27. Z. C. Wen, R. Yang, H. He, Y. B. Jiang, *Chem. Commun.* **2006**, *0*, 106.
28. M. M. Yu, W. W. Du, W. Zhou, H. X. Li, C. X. Liu, L. H. Wei, Z. X. Li, H. Y. Zhang, *Dyes Pigm.* **2016**, *126*, 279.
29. Z. Xu, Y.-Y. Ren, X. Fan, S. Cheng, Q. Xu, L. Xu, *Tetrahedron* **2015**, *71*, 5055.
30. H.-I. Un, S. Wu, C.-B. Huang, Z. Xu, L. Xu, *Chem. Commun.* **2015**, *51*, 3143.
31. C.-B. Huang, J. Huang, L. Xu, *RSC Adv.* **2015**, *5*, 13307.
32. H.-I. Un, C.-B. Huang, J. Huang, C. Huang, T. Jia, L. Xu, *Chem. Asian J.* **2014**, *9*, 3397.
33. H.-I. Un, C.-B. Huang, C. Huang, T. Jia, X.-L. Zhao, C.-H. Wang, L. Xu, H.-B. Yang, *Org. Chem. Front.* **2014**, *1*, 1083.
34. S. Xu, W. Li, K.-C. Chen, *Chin. J. Chem.* **2007**, *25*, 778.
35. L.-B. Li, S.-J. Ji, W.-H. Lu, *Chin. J. Chem.* **2008**, *26*, 417.
36. C. Yu, J. Zhang, *Asian J. Org. Chem.* **2014**, *3*, 1312.
37. Z. Chen, L. Wang, G. Zou, M. Teng, J. Yu, *Chin. J. Chem.* **2012**, *30*, 2844.
38. X. Poteau, A. I. Brown, R. G. Brown, C. Holmes, D. Matthew, *Dyes Pigm.* **2000**, *47*, 91.
39. L. H. Jia, Y. Zhang, X. F. Guo, X. H. Qian, *Tetrahedron Lett.* **2004**, *45*, 3969.
40. J. Liu, G. L. Tu, Q. G. Zhou, Y. X. Cheng, Y. H. Geng, L. X. Wang, D. G. Ma, X. B. Jing, F. S. Wang, *J. Mater. Sci.* **2006**, *16*, 1431.
41. W. H. Zhu, M. Hu, R. Yao, H. Tian, *J. Photochem. Photobiol. A: Chem.* **2003**, *154*, 169.
42. I. Grabchev, I. Moneva, V. Bojinov, S. Guittonneau, *J. Mater. Chem.* **2000**, *10*, 1291.
43. H. L. Mu, R. Gong, Q. Ma, Y. M. Sun, E. Q. Fu, *Tetrahedron Lett.* **2007**, *48*, 5525.
44. Y. J. Zheng, J. Orbulescu, X. J. Ji, F. M. Andreopoulos, S. M. Pham, R. M. Leblanc, *J. Am. Chem. Soc.* **2003**, *125*, 2680.
45. Y. Xiang, A. Tong, *Luminescence* **2008**, *23*, 28.
46. H. J. Kim, S. Y. Park, S. Yoon, J. S. Kim, *Tetrahedron* **2008**, *64*, 1294.
47. H. J. Kim, J. Hong, A. Hong, S. Ham, J. H. Lee, J. S. Kim, *Org. Lett.* **2008**, *10*, 1963.
48. W. Y. Lin, L. Yuan, W. Tan, J. B. Feng, L. L. Long, *Chem. A Eur. J.* **2009**, *15*, 1030.

49. S. Thavornpradit, J. Sirirak, N. Wanichacheva, *J. Photochem. Photobiol. A: Chem.* **2016**, *330*, 55.
50. Q. T. Meng, Y. Shi, C. P. Wang, H. M. Jia, X. Gao, R. Zhang, Y. F. Wang, Z. Q. Zhang, *Org. Biomol. Chem.* **2015**, *13*, 2918.
51. R. Zhang, X. J. Yu, Y. J. Yin, Z. Q. Ye, G. L. Wang, J. L. Yuan, *Anal. Chim. Acta* **2011**, *691*, 83.
52. M. H. Lim, B. A. Wong, W. H. Pitcock Jr.. , D. Mokshagundam, M. H. Baik, S. J. Lippard, *J. Am. Chem. Soc.* **2006**, *128*, 14364.
53. A. P. de Silva, H. Q. N. Gunaratne, J. -L. Habib-Jiwan, C. P. McCoy, T. E. Rice, J. -P. Soumillion, *Angew. Chem. Int. Ed.* **1995**, *34*, 1728.
54. N. I. Georgiev, A. M. Asiri, A. H. Qusti, K. A. Alamry, V. B. Bojinov, *Sens. Actuators B: Chem.* **2014**, *190*, 185.
55. M. D. McKenn, I. Grabchev, P. Bosch, *Dyes Pigm.* **2009**, *81*, 180.
56. N. I. Georgiev, V. B. Bojinov, N. Marinova, *Sens. Actuators B: Chem.* **2010**, *150*, 655.
57. N. V. Marinova, N. I. Georgiev, V. B. Bojinov, *J. Photochem. Photobiol. A: Chem.* **2013**, *254*, 54.
58. D. Staneva, I. Grabchev, R. Betcheva, *Dyes Pigm.* **2013**, *98*, 64.
59. S. Yordanov, I. Grabchev, S. Stoyanov, I. Petkov, *J. Photochem. Photobiol. A: Chem.* **2014**, *283*, 1.
60. D. Staneva, I. Grabchev, J. P. Soumillion, V. Bojinov, *J. Photochem. Photobiol. A: Chem.* **2007**, *189*, 192.
61. N. I. Georgiev, V. B. Bojinov, P. S. Nikolov, *Dyes Pigm.* **2011**, *88*, 350.
62. P. Job, *Ann. Chim. Appl.* **1928**, *9*, 113.
63. H. A. Benesi, J. H. Hildebrand, *J. Am. Chem. Soc.* **1949**, *71*, 2703.
64. F. Yu, W. S. Zhang, P. Li, Y. L. Xing, L. Tong, J. P. Ma, B. Tang, *Analyst* **2009**, *134*, 1826.
65. Y. Xiang, A. Tong, P. Y. Jin, Y. Ju, *Org. Lett.* **2006**, *8*, 2863.
66. S. P. Wu, K. J. Du, Y. M. Sung, *Dalton Trans.* **2010**, *39*, 4363.
67. G. H. Wu, D. X. Wang, D. Y. Wu, Y. Gao, Z. Q. Wang, *J. Chem. Sci.* **2009**, *121*, 543.
68. O. Stern, M. Volmer, *Z. Phys.* **1919**, *20*, 183.
69. H.-L. Wang, L. Yang, W.-B. Zhang, Y. Zhou, B. Zhao, X.-Y. Li, *Inorg. Chim. Acta* **2012**, *381*, 111.
70. S. D. Lytton, B. Mester, J. Libman, A. Shanzer, Z. I. Cabantehik, *Anal. Biochem.* **1992**, *205*, 326.
71. J. L. H. Jiwan, C. Branger, J. P. Soumillion, B. Valeur, *J. Photochem. Photobiol. A: Chem.* **1998**, *116*, 127.
72. S. Saha, A. Samanta, *J. Phys. Chem. A* **2002**, *106*, 4763.
73. V. B. Bojinov, N. I. Georgiev, P. S. Nikolov, *J. Photochem. Photobiol. A: Chem.* **2008**, *197*, 281.
74. Y. K. Tsui, S. Devaraj, Y. P. Yen, *Sens. Actuators B: Chem.* **2012**, *161*, 510.
75. C. G. Niu, G. M. Zeng, L. X. Chen, G. L. Shen, R. Q. Yu, *Analyst* **2004**, *129*, 20.

